Colloid Polym Sci (2005) 283: 954–967
DOI 10.1007/s00396-004-1243-8

Bin Shi
Chao Fang
Mei Xian You
Yan Zhang
Shoukuan Fu
YuanYing Pei

Stealth MePEG-PCL micelles: effects of polymer composition on micelle physicochemical characteristics, in vitro drug release, in vivo pharmacokinetics in rats and biodistribution in S_{180} tumor bearing mice

Received: 24 June 2004
Accepted: 2 November 2004
Published online: 22 December 2004

B. Shi · C. Fang · M. X. You
Y. Pei (✉)
School of Pharmacy of Fudan University, Shanghai, 200032, China
E-mail: sb750317@163.net
Tel.: +86-21-54237252
Fax: +86-21-54237186

Y. Zhang · S. Fu
Department of Macromolecular Science of Fudan University and the Key Laboratory of Molecular Engineering of Polymers, Ministry of Education, Shanghai, 200433, China

Abstract The amphiphilic copolymer of poly(methoxy-polyethyleneglycol polycaprolactone) (MePEG-PCL) was synthesized. Micelles loading hydroxycamptothecin (HCPT) as a model drug were prepared by solid-dispersion and dialysis–hydration method. The MePEG-PCL micelles were further characterized in terms of critical association concentrations (CAC), PEG surface density, fixed aqueous layer thickness, in vitro drug release and in vivo pharmacokinetics and biodistribution. The results showed that longer polycaprolactone (PCL) chain length would lead to the reduction of CAC value, stabilized HCPT, increasing drug-loading coefficient, sparser PEG surface density and slower drug release patterns. On the other hand, longer PEG chain length would give rise to less negative zeta potential and larger fixed aqueous layer thickness, as well as sparser PEG surface density and quicker drug release. MePEG-PCL micelles with PEG molecular weight of 2,000, 5,000, 10,000 could extend the AUC of HCPT in blood compartment by 9.13, 13.82, 21.25 times and increase the AUC of ^{125}I-HCPT in the tumor of S_{180} mice by 7.94, 11.32, 26.08-fold, respectively. It was suggested that the PEG and PCL chain length may play a very important role in the micelle's in vitro properties and in vivo behavior.

Keywords Poly(methoxy-polyethyleneglycol polycaprolactone) · Micelle surface properties · Hydrocamptothecin · Pharmacokenitics · Biodistribution

Introduction

Micelles or colloidal carriers have been widely studied for targeted drug delivery and other biomedical application, especially for anticancer drugs [1, 2]. Encapsulation of active compounds into polymeric carriers represents a very promising way of increasing drug bioavailability, preventing drug degradation, reducing drug toxic effects, controlling drug release and achieving specfic targeting [3]. However, the therapeutic potentialities of injectable particulate drug carriers (polymeric nanoparticles and liposomes) may be compromised by opsonins adsorption and subsequent particle recognition by the macrophages of the mononuclear phagocyte system [4]. Thus, a threshold of nanoparticle size smaller than 200 nm and a hydrophilic surface (as opposed to the hydrophobic surface of conventional nanoparticles) are needed, in order to reduce opsonization reactions and subsequent clearance by macrophages [5].

Micelles as drug carriers are able to provide a series of unbeatable advantages—they can solubilize poorly soluble drugs by hydrophobic core resulting in the increase of drug stability and bioavailability. They can stay in the body long enough providing gradual accumulation in the required area. Their size (about 50–200 nm) permits them to accumulate in body regions with leaky vasculature [6], and they can be targeted by attachment of a specific ligand to the outer surface [7].

The drugs loaded in the micelles can be well protected from possible inactivation under the effect of biological surroundings, and their bioavailability are usually increased.

In the literature, a number of amphiphilic copolymers were reported, such as poly(methoxypolyethyleneglycol cyanoacrylate-*co*-hexadecyl cyanoacrylate) (MePEG-PHDCA) [8, 9], poly(*N*-isopropylacrylamide)-*b*-polyethyleneglycol [10], poly(aspartic acid)-*b*-polyethyleneglycol (PAA-PEG) [11], poly(D,L-lactide)-*b*-methoxypolyethyleneglycol [12] and poly(*r*-benzyle-*l*-glutamate)-*b*-polyethyleneglycol [13]. These copolymers can disintegrate into biocompatible and non-toxic unimers that will be easily cleared from the body. More recently, the possibility of developing biodegradable PEG-coated nanoparticles has been considered by using polycaprolactone-*b*-polyethyleneglycol (PCL-PEG) and both in vitro and in vivo experiments showed the ''stealth'' properties of the nanoparticles prepared from this material [14]. Furthermore, the methoxy poly(ethylene glycol)/poly(ε-caprolactone) diblock copolymeric nanosphere encapsulating indomethacin could extend the half-life of the drug to 23.1 h (about two times that of free indomethacin) [15]. The results of these studies provided fundamental information on the long-circulating properties of MePEG-PCL nanoparticles. However, no reports have been made about the interaction between nanoparticle physicochemical properties and in vivo behavior so far.

It was well recognized that particle size [16–18], the zeta potential, the PEG chain length [19], the PEG surface density [20] and fixed aqueous layer thickness (FALT) [21] of the nanoparticles played an essential role in nanoparticles' in vitro and in vivo behaviors. As far as the ''stealth'' properties of the nanoparticles are concerned, particles smaller than 200 nm in size and a slight negative or neutral zeta potential were needed [22], for particles bigger than 200 nm or with strong negative zeta potential would be easily recognized by the macrophages of the mononuclear phagocyte system and rapidly eliminated from the blood stream. Second, the hydrophilic surface of nanoparticles (such as PEG) was needed. Gref et al. [19] confirmed that the plasma protein adsorption and phagocytic uptake could be prevented by the PEG coating of poly(lactide) (PLA), poly(lactide-*co*-glycolide) (PLGA) and poly(caprolactone) (PCL) nanoparticles, and a maximal reduction in protein adsorption was found for a PEG Mw of 5,000 g/mol. Furthermore, Bazile et al. [22] suggested that a grafting surface density close to 1.5–2 nm^2/PEG molecule for one PEG was optimal for avoiding complement consumption, corresponding to a distance of 1.2–1.4 nm between two grafted PEG2000 chains. Other authors suggested that 2.2 nm was the maximum distance for avoiding complement consumption [23]. Besides, fixed aqueous layer thickness (FALT) of PEG-modified nanoparticles was measured by Sadzuka, proving that FALT could prevent the attraction of opsonins and avoid trapping by mononuclear phagocyte system [21]. However, most of the data were got from the nanoparticles with no drug loaded. In order to investigate how these parameters interacted with each other and contributed to in vivo pharmacokinetics and biodistribution, in this study, we synthesized MePEG-PCL copolymers of different PEG chain length and different molar ratio of PEG to PCL. And we attempted to load anticancer drugs, 10-hydroxycamptothecin (HCPT), as a probe drug.

The HCPT a novel camptothecin (CPT) congener widely used in China, has shown more powerful antitumor activity to lung, ovarian, breast, pancreas and stomach cancers than CPT [24]. However, it was shown that HCPT had some practical disadvantages in clinical use mainly due to (a) poor water solubility, (b) a number of toxic effects, (c) in vitro and in vivo instability, (d) shorter half-life in vivo. In an attempt to establish the optimal schedule of administration, numerous trials have been conducted. It was shown that the HCPT require a prolonged schedule of administration given continuously at low doses or frequent fractioned dosing schedules to spare normal hematopoietic cells and mucosal progenitor cells with low topoisomerase-I levels while preserving efficacy [25, 26]. In the light of this, the development of controlled delivery formulations seemed to be a promising strategy, in which the micelles are highlighted for their capability to solubilize hydrophobic drugs and increase their circulation time [27, 28]. To solve this problem, micelles using MePEG-PCL as carrier material and hydrocamptothecin as a model drug were prepared. The physicochemical properties of core-shell type micelles (particle surface properties in particular), drug release profile, pharmacokinetic characteristics in rats and biodistribution in S_{180} tumor bearing mice were investigated, and the influences of chain length of PEG on micelle surface properties and in vivo pharmacokinetics and biodistribution were discussed.

Experimental

Materials

Methoxy-polyethyleneglycol (MePEG), (MW = 2 and 5 kDa), pyrene and stannousoctoate (SnOct) was purchased from Sigma Chem.Co., (USA). MePEG (MW = 10 kDa) was provided by the Department of Macromolecular Science, of Fudan University. All PEG was dehydrated by azeotropic distillation with toluene. ε-CL (from Aldrich) was dried over phosphorus pentoxide for 48 h at room temperature and then distilled underreduced pressure prior to polymerization. HCPT was purchased from Shanghai Fudan Taxusal New

Technology Corp of China. All other chemicals and solvents were of reagent grade and the solvents were dehydrated with a molecular sieve.

Animals

Male Wistar rats (200 ± 20 g) and S_{180} tumor bearing Kunming mice (25 ± 5 g) were supplied by the Shanghai Experimental Animal Center, Chinese Academy of Sciences (Shanghai, China). The animals were acclimatized at a temperature of 25 ± 2 °C and a relative humidity of $70 \pm 5\%$ under natural light/dark conditions for 1 week before dosing.

Preparation of HCPT-loaded polymer micelles

An amount of 50 mg MePEG-PCL was dissolved in 5 ml tetrahydrofuran (THF) and then the solution was added to 30 ml stirred water with a syringe. The solution formed was dialyzed with molecular cutoff (MWCO) 14,000 g/mol dialysis bag against 1,000 ml water for 24 h during which the distilled water was exchanged at intervals of 0.5 h. HCPT-span solid dispersion was made by solvent evaporation method. A predetermined amount of HCPT and span60 were dissolved in THF, and then evaporated by the Rotavapor R-200 (Buchi, USA). Finally, certain amount of MePEG-PCL solution was put into the solid dispersion and hydrated at 70 °C for 20 min under stirring, and then, the solution was filtered through 0.85 μm cellulose acetate filter membrane to remove the drug crystals and the copolymer aggregates. The micelle solution was lyophilized.

Determination of drug loading parameters

Hydroxycamptothecin was extracted from the MePCL-PEG micelles with dimethyl sulfoxide (DMSO). Micelles were immersed in excess DMSO and vigorously vortexed. The solution was properly diluted prior to HPLC analysis. Drug loading coefficient (DL) and encapsulation ratio (ER) were calculated as following:

$$\mathrm{DL}\% = \frac{\text{Weight of the drug in micelles}}{\text{Weight of the feeding polymer and drug}} \times 100\% \quad (1)$$

$$\mathrm{ER}\% = \frac{\text{Weight of the drug in micelles}}{\text{Weight of the feeding drug}} \times 100\% \quad (2)$$

Furthermore, the core molecular weight of PCL could be estimated with the composition of MePEG-PCL obtained by ^{1}H-NMR. By comparing the weight of the drug encapsulated with that of PCL, we introduced hydrophobic interaction coefficient (HIC):

$$\mathrm{HIC} = \frac{\text{Weight of the drug}}{\text{Weight of the PCL}} \quad (3)$$

HIC value would be useful for evaluating the hydrophobic interaction and compatibility between the drug and hydrophobic part of copolymer.

HPLC methods for determination of HCPT both in vitro or in vivo

The HPLC determination of HCPT in vitro experiment was performed using a pharmacia gradient chromatographic pump, a LC-10ATVP Shimadzu chromatographic sample injection valve equipped with a 20 μl loop and a Shimadzu UV detector. Samples were chromatographed on a 150×4.6 mm reverse phase stainless steel column packed with 5 μm particles (Hypersil ODS, USA), eluted isocratically at room temperature with a mobile phase consisting of 65:35 mixture of aqueous triethylamine–acetate buffer (pH 5.5) and acetonitrile. The flow rate was set at 0.55 ml/min and HCPT was monitored at 368 nm [24].

The amount of HCPT in plasma was extracted as follows. Once the blood sample was drawn, it was immediately placed on ice and centrifuged at 400*g* for 10 min at 4 °C. The plasma was frozen at −25 °C until assay. 10 μl of phosphorous acid, 200 μl of CPT as internal standard and 1.5 ml of ethyl acetate were added into 200 μl of plasma and vortexed for 2 min. The mixture was sonicated for 5 min and centrifuged at 5,000*g* for 5 min. The clear supernatant of 1 ml was dried under nitrogen and dissolved in 200 μl methanol and centrifuged at 5,000×*g* for 5 min before HPLC analysis. HPLC condition was the same as above except that at room temperature, the mobile phase consisted of A (acetonitrile) and B (aqueous triethylamine–acetate buffer (pH5.5) was used with gradient elution of A:B (20:80) and A:B (55:45) from 0∼10 min with a flow rate at 0.85 ml/min. HCPT was monitored by a fluorescence detector with excitation wavelength at 368 nm and emission wavelength at 550 nm.

Characterization of micelles

The structure of MePEG-PCL micelle

The surface morphology was evaluated by transmission electron microscopy (TEM, Philips CM120). In practice, a drop of micelle suspension containing 0.1 wt% phosphotungstic acids was placed on a carbon film coated on a copper grid and observed at 80 kV in the electron microscopy. The micelle size and distribution were

determined with a laser diffraction particle size analyzer (NicompTM 380ZLS zeta potential/particle sizer).

Critical association concentrations of the MePEG-PCL copolymers

To estimate the critical association concentrations (CAC) of MePEG-PCL copolymers, pyrene was used as a hydrophobic probe [29, 30]. To obtain sample solutions, a known amount of pyrene in acetone was added to a series of 20 ml vial and the acetone was evaporated under nitrogen. The final concentration of pyrene was 5.0×10^{-7} mol/l. After 10 ml of various concentrations of copolymer solutions was added, each vial was set for 5 h at 65 °C to equilibrate the pyrene and the graft copolymer solution and left to cool overnight at room temperature. Emission wavelength was 393 nm and excitation wavelength was 335 and 338 nm. Excitation and emission bandwidth was 5 and 5 nm, respectively. In the point of CAC, pyrene fluorescence emission spectra would show a dramatic change at I_{338}/I_{335}.

Zeta potential and the fixed aqueous layer thickness of the micelles

The zeta potential of the micelles was measured in water by zeta potential/particle size. The fixed aqueous layer thickness of the micelles was calculated using Gouy–Chapmann theory [21]. According to this theory, zeta potential $\psi[L]$ as the electrostatic potential at the position of the slipping plane L (nm) is expressed as:

$$\ln \psi[L] = \ln A - kL \tag{4}$$

where A is regarded as a constant and k is the Debye–Huckel parameter, equal to $\sqrt{c/0.3}$ (c is the molality of electrolytes) for universal salts. If zeta potentials are measured from the changing concentration of NaCl (namely 0, 10, 50 and 100 Mm) and plotted against k, the slope L gives the position of the slipping plane or thickness of the fixed aqueous layer in nanometer units.

PEG surface density

The PEG concentration was measured by a colorimetric assay. Briefly, standards (0–6 μg PEG/ml) and samples were diluted with 3.0 ml of water and mixed with 75 μl of a mixture composed of I_2 (10 g/l) and KI (20 g/l); the samples hydrolyzed by NaOH (2 N, 50 °C, 5 days) were neutralized with 1 N HCl. Absorbance was read at 525 nm. Calculation of the average PEG surface density were made as follows [31]:

$$\delta = \frac{N \times d \times \alpha \times r}{3\mathrm{MW_{PEG}}} \tag{5}$$

where δ is the surface density of PEG chains (PEG/nm^2), N is the Avogadro number, r is the particle radius neglecting the PEG layer thickness (error $<10\%$), d is the density of micelles, α is the total PEG content after micelles degradation and $\mathrm{MW_{PEG}}$ stands for molecular weight of PEG.

From the data of surface density of PEG chains, the average distance D between two neighboring PEG could be obtained:

$$D = \sqrt{\frac{1}{\delta}} \tag{6}$$

In vitro release studies

To measure how fast the drug was released in the different formulation of micelles, samples of 30 mg of micelles were suspended in 1,000 ml of phosphate buffer saline (PBS) (pH 7.4) containing 1% (w/v) tween 80 and incubated at 37 °C under gentle magnetic stirring at 100 rpm. Micelles were placed in dialysis bags and at predetermined time intervals, 5 ml samples were withdrawn and acidified with 1 N HCl, and the total amount of HCPT in the supernatant was determined by HPLC method. To evaluate what form of HCPT was actually released from the micelles, the PBS buffer was replaced at frequent time intervals to characterize the form of the drug. Practically, the micelles were exposed to PBS (pH 6.5) for 10 min and the released HCPT was immediately analyzed before significant lactone–carboxylate conversion. Concentrations of both active lactone and carboxylate forms of HCPT in the release media were determined by HPLC method. Each micelle batch was analyzed in triplicate.

Pharmacokinetics of micelles in rats

Four groups of male Wistar rats ($n=6$) were used in this experiment, group 1 being treated with HCPT solution, group 2–4 with $\mathrm{MePEG_{2,000}}$-PCL(1:6), $\mathrm{MePEG_{5,000}}$-PCL(1:8), $\mathrm{MePEG_{10,000}}$-PCL(1:8) micelles, respectively. For administration, micelles were dispersed in a certain volume of NaCl (0.9%) in order to obtain the required concentration. Simultaneously, a solution of HCPT in the same vehicle with the same concentration was prepared by diluting HCPT injection. Each animal was dosed intravenously with 2.5 mg HCPT/kg.

After intravenous administration, blood was collected at 0.083, 0.25, 0.5, 1, 2, 4, 8, 12, 24 h from the tail vein and the HCPT concentration was measured.

Biodistribution of ^{125}I-HCPT-loaded micelles in mice

HCPT labeled with ^{125}I was prepared by the procedure as follows: 330 μg of HCPT in 100 μl methanol was

layered over a freshly prepared film of IODO-GEN (100 μg) and incubated for 5 min at 4 °C for 10 min in the presence of 2 mCi of $Na^{125}I$. The reaction mixture was transferred to another tube and detected with HPLC system to measure the purity of ^{125}I-HCPT. HPLC condition: a SPD-10A VP Shimadzu HPLC equipped with a UV and radioactivity detector. Samples were chromatographed on a 250×4.6 mm reverse phase stainless steel column packed with 5 μm particles (Hypersil ODS, USA). At room temperature, the mobile phase consisted of A (0.1% trifluoroacetic acid and acetonitrile) and B (0.1% trifluoroacetic acid and water) was used with gradient elution of A 0∼100% and B 100∼0% from 0∼20 min with a flow rate at 1.0 ml/min.

The micelles containing ^{125}I-HCPT were prepared by solid-dispersion and dialysis–hydration method, and then centrifuged and washed, and the supernatants were assessed for gamma emission. The amount of ^{125}I-HCPT encapsulated into the micelles was calculated by the difference between the total amount used to prepare the micelles and the amount of ^{125}I-HCPT present in the aqueous phase.

S_{180} tumor bearing mice, body weight between 20 g and 25 g, were used for body distribution studies and given KI for 1 week. The mice, three per group, were injected at random in the tail vein with 200 μl micelles (9.375 μCi per mouse) and 200 μl ^{125}I-HCPT solution in 0.9% NaCl solution. At the predetermined time, blood samples were collected from the ocular artery after eyeball removal. And then the mice were sacrificed, and their tissues (tumor, heart, liver, spleen, lung, kidney) were excised, washed quickly with cold water to remove surface blood, and counted for radioactivity. The biodistribution experiments adhered to the ''Principles of Laboratory Animal Care'' (NIH publication#85-23, revised 1985).

Statistical analysis

The in vivo pharmacokinetics and biodistribution results were evaluated for statistical significance with the Student's t test, analysis of variance (ANOVA) and the Dunnett t tests (two-sides) using SPSS10.0 for windows. A p-value below 0.05 was considered significant.

Results and discussion

The structure of MePEG-PCL micelle and CAC value

From Fig. 1, the TEM image of micelles made of $MePEG_{5,000}$-PCL (1:8) showed that the micelles had uniform size and were round in shape.

The formation of core-shell type structures of MePEG-PCL was further confirmed by a fluorescence probe technique applying pyrene as a hydrophobic probe. Figure 2a showed the excitation spectra of pyrene in various concentrations of MePEG-PCL copolymer. Pyrene would be partitioned into hydrophobic cores with the change of surrounding environment. In very low concentrations of MePEG-PCL below CAC, the marker of pyrene was dissolved in a polar environment of water and fluorescence intensity in I_{338}/I_{335} was very low. However, in the presence of micelles, a hydrophobic micelle core solubilizing pyrene resulted in an increase of fluorescence intensity in I_{338}/I_{335}. In Fig. 2a, a red shift was observed with increasing concentration of MePEG-PCL copolymer. And the rise of ratio I_{338}/I_{335} versus log C was shown in Fig. 2b. In the lower concentration, there was a flat region. While in the region of 0.007813 g/L the signal rose dramatically, indicating that the micelles of MePEG-PCL copolymer had begun to form. As shown in Table 1, CAC value of MePEG-PCL was decreased with the increase of PCL chain length. It is known that the stability of micelles both in vitro and in vivo depends on the CAC values. Upon dilution to CAC, micelles would begin to dissociate into unimers and thus release drugs. In general, the lower the CAC value, the better the micelle stability.

From the thermodynamics point of view, the solubilization of the drug can be considered as a normal

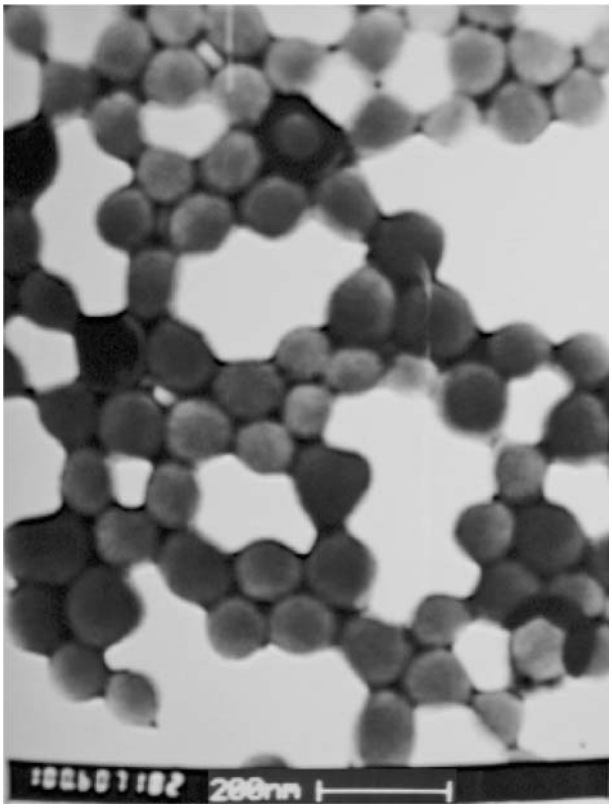

Fig. 1 The TEM figure of MePEG-PCL micelle

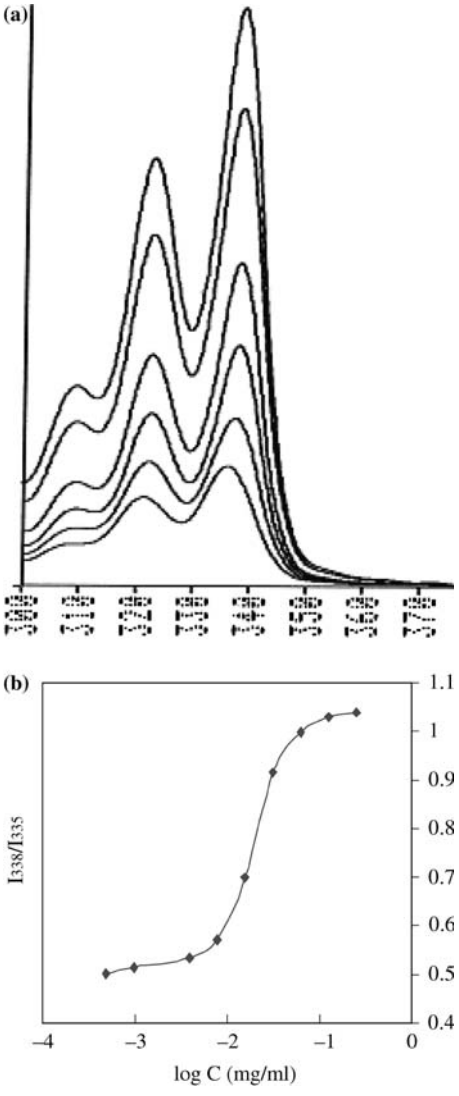

Fig. 2 **a** Fluorescence excitation spectra of perene (5.0×10^{-7} mol/L) against MePEG-PCL concentration in distilled water (emission wavelength 393 nm) and **b** plot of the intensity ratio I_{338}/I_{335} from pyrene exitation spectra versus log C (g/L) of $MePEG_{5,000}$-PCL (1:1) in distilled water

partitioning of the drug between two phases, micellar and aqueous, and the standard free energy of solubilization (ΔG) can be experessed via the corresponding partition coefficient according to Torchilin [1]:

$$\Delta G = -RT \ln \text{CAC} \tag{7}$$

From Table 1, the data showed that all MePEG-PCL micelles had negative free energy, so they must be self-assembling systems and thermodynamically stable.

The drug-loading process and parameters of MePEG-PCL micelles

It was observed that in Table 2, with the increase of molecular weight of MePEG-PCL and drug loading, the particle size increased correspondingly. However, the increase of PEG chain length with the similar PCL chain length seemed to produce a smaller particle size (observed between $MePEG_{5,000}$-PCL (1:16) and $MePEG_{10,000}$-PCL (1:8), between $MePEG_{5,000}$-PCL (1:8) and $MePEG_{10,000}$-PCL (1:4), between $MePEG_{5,000}$-PCL (1:2) and $MePEG_{2,000}$-PCL (1:6)). This was understandable because PEG was able to moderate the association of the copolymer molecules during the formation of the particles, as reported by Riley et al. in 1999 [34]. Second, both the increase of PEG length and PCL length contributed to the increase of drug loading. It is well recognized that with the increase of the hydrophobic part of the copolymer, the drug-loading coefficient would rise. And this could be observed in Fig. 3a. With the PCL ratio increased, the drug loading coefficient rose significantly. In order to evaluate the hydrophobic interaction and compatibility between the drug and hydrophobic part of copolymer more conveniently, we introduced the concept of hydrophobic interaction coefficient:

$$\text{HIC} = \frac{W_{\text{drug}}}{W_{\text{PCL}}} \tag{8}$$

The higher the HIC value, the better the compatibility between drug and copolymer. As shown in Fig. 3b, hydrophobic reaction coefficient was increased with both

Table 1 CAC, FALT and ΔG of copolymer MePEG-PCL of different PEG and PCL chain lengths

Micelle	CAC[b] ($\times10^7$ mol/L)	ΔG[c] (kJ/mol)	FALT[d] (nm)	Zeta potential (mV)
NP5K11[a]	7.5	−34.93	4.32	−6.5 ± 1.2
NP5K12	2.7	−37.44	4.20	−6.7 ± 1.3
NP5K14	1.1	−39.64	4.15	−6.9 ± 0.9
NP5K18	0.4	−41.95	4.04	−6.8 ± 1.4
NP10K18	0.1	−45.14	7.13	−1.2 ± 0.3
NP2K16	8.7	−34.59	3.82	−10.3 ± 2.3

[a]NP5K11 means the micelle was made of the copolymer of P5K11, namely $MePEG_{5,000}$-PCL(1:1)
[b]CAC was the critical association concentrations
[c]ΔG was the free energy of solubilization
[d]FALT was the fixed aqueous layer thickness

Table 2 Drug-loading parameter of MePEG-PCL micelles and in vitro characterization

Nano particle	DL (%)	ER (%)	Size[a] (nm)	Size[b] (nm)	δ[c] (PEG/nm^2)	D[d] (nm)	HCPT[e] (%)
NP5K11	1.32	73.20	25.3 ± 2.0	47.5 ± 20.0	0.49	1.42	88.87
NP5K12	1.84	65.35	44.2 ± 8.7	51.5 ± 20.1	0.48	1.45	89.14
NP5K14	2.49	62.81	55.9 ± 22.9	75.2 ± 13.2	0.39	1.60	94.04
NP5K18	4.22	75.18	75.5 ± 9.3	84.2 ± 10.7	0.38	1.62	97.31
NP5K116	6.17	71.36	96.4 ± 23.4	99.2 ± 30.0	0.36	1.67	97.38
NP2K14	1.54	69.93	36.0 ± 4.5	44.5 ± 5.8	0.59	1.30	86.17
NP2K16	2.00	69.61	59.5 ± 6.4	65.6 ± 8.1	0.56	1.34	96.95
NP10K14	4.11	69.36	63.2 ± 22.9	77.3 ± 13.7	0.28	1.89	97.99
NP10K18	6.77	68.41	81.3 ± 30.5	82.7 ± 30.6	0.18	2.35	97.29

[a]The particle size before drug loading
[b]The particle size after drug loading
[c]δ is the surface density of PEG chains
[d]D is the average distance between two neighboring PEG
[e]The ratio of lactone form of the HCPT in the micelle

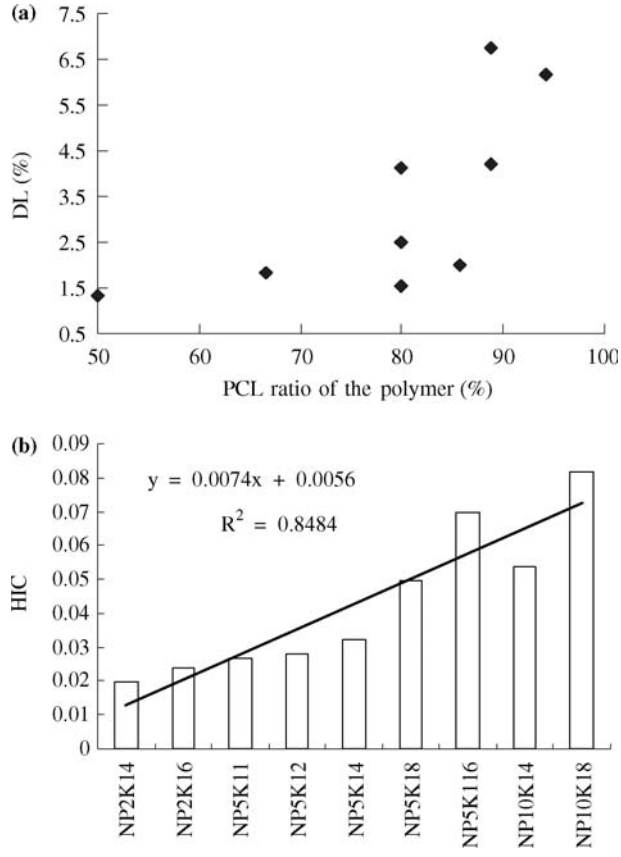

Fig. 3 **a** The drug-loading coefficient against the PCL ratio of the copolymer and **b** the HIC value against different types of MePEG-PCL copolymer

PCL ratio of the polymer and MePEG-PCL molecular weight of the polymer. We conjectured that as PEG length increased, the micelle seemed to be more stabilized in the drug-loading process. This result is not consistent with our result got from PEG-PHDCA, a type of copolymer, which can form star-shape micelles. This is because the MePEG-PCL copolymer has a more tight structure due to the longer PCL chain length. To illustrate the roles that PEG chain length and PCL chain length played in the drug-loading process, we further analyzed it by linear regression of SPSS. The result confirmed that the hydrophobic interaction coefficient was mainly influenced by the PCL chain length in micelle core and slightly influenced by the outer PEG chain length.

And last but most important, from the pharmacological aspect, we further evaluate the stability of the drug during the drug-loading process. It is well known that a closed hydroxylactone moiety of HCPT is essential for maintaining its interaction with the topoisomerase-I target and antitumor potency in vivo. When the lactone form of HCPT is converted to inactive carboxylate form, most of its efficacy will be lost. As shown in Table 2, HCPT loaded in the micelles was mostly stabilized as the lactone form of the drug (all formulation $>85\%$). And with the increase of PCL chain length, the effect of drug-protection was also raised.

The drug-loading coefficient was mainly influenced by the following factors: the affinity of the drug with the core chain length, the size of the hydrophobic core, drug solubility in water and drug–drug interaction. The most important factor among them is the compatibility between the drug and the core block. As HCPT has a poor solubility in most organic solvents, a low affinity with PLA, PCL or their copolymers, and a strong tendency to self-aggregate, their loading content in micelles is far from satisfactory. Based on observation, the drug-loading content of HCPT or CPT in MePEG-PCL prepared by dialysis method could hardly exceed 1%. This result was quite consistent with that of Zhang [32]. Therefore, we ventured on different methods for raising the drug-loading coefficient. Through the experiment of HCPT solubility in a number of lipid, we found that span60 had a good compatibility with the drug. Span60 was reported to form a niosome structure with particle size ranging from 1 μm to 10 μm [33]. However, in this formulation, it could hardly form niosomes, for MePEG-PCL had too long a hydrophobic chain length which destroyed the lipid bilayer of span60. The addition of span60 added might increase the compatibility

between the drug and micelle core and expand the space of hydrophobic core of MePEG-PCL, which made it more applicable for loading a specific drug. This phenomenon was also reported in a number of micelles [1].

The structure of HCPT-span loaded MePEG-PCL was shown in Fig. 1, indicating that the micelles had uniform size and no niosome was formed during the preparation process. Further, it should be mentioned that the copolymer of MePEG-PCL could not be well dispersed in water without the dialysis process (except the MePEG-PCL(1:1) copolymer). Secondly, taking into consideration that the temperature of 70 °C used in hydration process is above the melting temperature of MePEG-PCL (about 50–70 °C) and span (about 52 °C, data got from DSC), and that HCPT was molecularly dispersed in span, when the formulation was heated in 70 °C under stirring, the mixture of MePEG-PCL, span and HCPT could take the chance to interact with each other adequately. When the temperature was lowered below their melting point, the MePEG-PCL and span began to crystallize and load the drug in its rigid core when PEG still remained in a liquid state in aqueous environment. And finally the unloaded HCPT crystals and other aggregates could be removed by filtrating through 0.85 μm cellulose acetate filter membrane.

The fixed aqueous layer thickness of the micelles

From Table 1, the surface negative charge of MePEG-PCL micelles dramatically decreased with the increasing PEG chain length. This may have been related to the PEG-aqueous layer. According to Gouy–Chapmann theory, the hydrodynamic drag caused by the PEG chains on the micelle surface moved the hydrodynamic plane of shear away from the charge-bearing plane, and therefore reduced the electrophoretic mobilities instead of the electrostatic surface potential.

It was well known that the negative zeta potential would facilitate the recognition of micelle by the macrophages of the mononuclear phagocyte system [35]. Therefore it was necessary for the long-circulating micelles to have a less negative or even neutral zeta potential. In this study, the steeper negativity reduction of MePEG-PCL with increasing NaCl concentration was explained quantatively by measuring the fixed aqueous layer thickness. It was observed that with increasing NaCl concentration, the longer the PEG chain length, the more steeply the absolute value of zeta potential of micelles decreased. And based on Gouy–Chapmann theory, the thickness of the fixed aqueous layer of MePEG-PCL was calculated in Table 1. The longer PEG chain length exhibited higher thickness of aqueous layer, which facilitated the micelles' stabilization. However, it should be mentioned that higher concentration of NaCl could also reduce the solvency power of water for PEG. When the concentration of the electrolyte was raised, the van der Waals attraction between the PCL core would exceed the surface charge repulsion. And while the PEG chains become dehydrated in higher concentration of NaCl, micelle flocculation occurs [36]. Therefore, this test should be carried out in the concentration of NaCl no more than 100 mM to prevent flocculation.

At last, according to modeling of PEG–lipid by Needham [37], it was suggested that MePEG-PCL constructed more complete 'mushroom' structures than 'brushes' structures, for in the 'brush' model, the micelles should have thicker FALT. With PEG on the micelle surface and formation of the fixed aqueous layers, it would be possible for the micelles to prevent the attraction of opsonins, avoid the serum proteins binding and escape the trapping by the cells of mononuclear phagocyte system [21].

PEG surface density

In the proposed model of MePEG-PCL micelles based on the measurement of PEG in different micelle fractions, a grafting surface density of 0.49, 0.48, 0.39, 0.38, 0.36 PEG/nm^2 was found for micelles of same PEG5000 chain length and increasing PCL chain length, indicating that the increase of PCL chain would have a negative effect on the PEG surface density (shown in Table 2). This might be due to the strengthened hydrophobic interaction between PCL length, which involved less molecular number of MePEG-PCL to shape a single micelle. It is understandable that the corresponding distance between two PEG chains was increasing at the same time. This could also explain the reduction of FALT with the increase in PCL chain length of MePEG$_{5,000}$-PCL. The decrease of PEG surface density could also be observed by increasing PEG chain length. When PEG chain length amounted to 10,000, the distance between two PEG chains was expanded. It was reported that PEG was able to moderate the association of the copolymer molecules during the formation of the particles by Riley et al. in 1999 [34]. Thus, it could be estimated that longer PEGs chain need more space to retain their flexibility, which made the surface PEG sparser. The flexibility of the PEG chain length was essential for them to escape the cells of the mononuclear phagocyte system. The reported data showed that a certain range of PEG surface density was needed for maintaining its flexibility [19]. These values could be very useful to evaluate the in vivo behavior of the MePEG-PCL micelles.

In vitro release

The aim of in vitro release of HCPT in MePEG-PCL could be defined as follows: first, what form of drug was

actually released from the micelles; second, how fast the drug was released. As reported by Shenderova [38], the stability of HCPT in the micelles was evaluated by two methods: (1) by extracting the drug from the micelles and (2) by capturing the HCPT in the release media before significant lactone–carboxylate conversion could take place. Examination of drug content from the micelles was described previously in the drug-loading process. And we confirmed that more than 85% drug was stabilized in the form of lactone. To evaluate drug composition by method (2), we chose PBS pH 6.5 for the lactone–carboxylate conversion rate was minimal at this pH (e.g., $t_{1/2} = 89$ min at pH 6.5, compared to $t_{1/2} = 21$ min at pH 7.4, data got from Burke et al. [39]). Control experiments were conducted to ensure that no significant conversion took place within 10 min of exposure to PBS pH 6.5 (< 8% drug converts in this time interval).

Table 3 showed that during drug release studies in PBS, initially 82–95% of HCPT were released in its lactone form from $MePEG_{5,000}$-PCL (1:2) to $MePEG_{10,000}$-PCL (1:8) micelles, indicating that most drugs were stabilized by the encapsulation of the micelle. The potential mechanisms of HCPT stabilization by MePEG-PCL are multifaceted. Although the degradation speed of MePEG-PCL micelles would be increased, compared to PCL microspheres (as reported by Ryu [29], PEG8000-PCL could be degraded to 7.5% in 10 days), the presence of a low microenvironmental pH to prevent hydrolysis of HCPT lactone would be very limited. Instead, it would be more practical that some interaction between the drug and polymer phase existed. It was conceivable that the active E-ring may be protected from hydrolysis by the increase of solubility of lactone form of the drug in the polymer phase compared with the water phase. Preferential partitioning of the lactone form into lipid bilayers has been previously reported to have a stabilizing effect for CPT [39]. And insufficient water in the nanoparticles interior could be another reason for HCPT stabilization, which would greatly reduce the rate of hydrolysis. It is likely that in order for HCPT lactone to be hydrolyzed, it should first be solubilized. Furthermore, the crystals formed in the core of the micelles was likely to be very stable and the conversion of lactone to carboxylate in the solid state is quite slow.

The factors influencing drug release speed include: (a) the release media used; (b) the characteristics of the copolymer; (c) the particle size and internal structure of the micelles; (d) the form of the drug loaded in the micelles. In this test, we fixed the release media as pH 7.4 PBS in order to investigate the other factors concerned. Firstly, the highest initial burst of HCPT solution from the dialysis bag with a cutoff of 14,000 (namely 100% in 6 h) was observed, indicating that the release lag time induced by the dialysis bag could almost be neglected. In Fig. 4, it was showed that the release kinetics of HCPT from the MePEG-PCL micelles against the different chain length of PCL and PEG. HCPT was continually released in vitro in 5 days without obvious burst release and the release pattern could be best fitted by Higuchi equation (Table 3). We had discovered that, as far as the MePEG-PHDCA copolymer is concerned, the higher the chain length of PEG, the faster the drug release kinetics. This could also be observed in PEG-PHDCA, irrespective of their different micelle structure. When the HCPT in $MePEG_{5,000}$-PCL (1:16) was released by 70%, $MePEG_{10,000}$-PCL (1:8) released the drug for 80%

Table 3 The release ratio of HCPT from MePEG-PCL against time by two regression models and release of active HCPT-lactone from MePCL-PEG micelles

Micelle	Higuchi equation	R	Peppas model	R	
HCPT release ratio from MePEG-PCL					
NP2K16	$Q = 10.613t^{1/2} - 11.845$	0.9935	$\log Q = 0.7564 \log t + 0.4966$	0.9968	
NP5K12	$Q = 10.635t^{1/2} - 13.786$	0.9935	$\log Q = 0.8161 \log t + 0.3744$	0.9972	
NP5K14	$Q = 9.7937t^{1/2} - 9.5193$	0.9915	$\log Q = 0.694 \log t + 0.5724$	0.9890	
NP5K18	$Q = 9.7018t^{1/2} - 12.29$	0.9814	$\log Q = 0.8465 \log t + 0.2792$	0.9882	
NP5K116	$Q = 7.6802t^{1/2} - 11.263$	0.9892	$\log Q = 0.904 \log t + 0.0485$	0.9878	
NP10K18	$Q = 8.6882t^{1/2} - 9.2691$	0.9870	$\log Q = 0.8685 \log t + 0.235$	0.9918	
	Time (days)				
	1	2	3	4	5
Release of HCPT-lactone from MePCL-PEG					
NP2K16	93.21 ± 0.52	92.11 ± 0.92	92.12 ± 0.35	91.21 ± 3.24	90.24 ± 0.35
NP5K12	85.34 ± 0.33	84.59 ± 0.25	84.23 ± 2.51	83.22 ± 0.25	82.24 ± 0.53
NP5K14	91.46 ± 0.12	90.16 ± 0.35	91.57 ± 2.58	90.26 ± 0.84	90.25 ± 1.23
NP5K18	94.21 ± 0.98	93.54 ± 0.26	93.69 ± 2.35	92.15 ± 1.59	91.59 ± 0.28
NP5K116	94.98 ± 0.57	94.26 ± 0.95	94.63 ± 2.13	93.29 ± 0.78	93.26 ± 0.25
NP10K18	95.12 ± 0.39	94.58 ± 0.46	94.65 ± 2.89	94.68 ± 2.33	93.68 ± 0.58

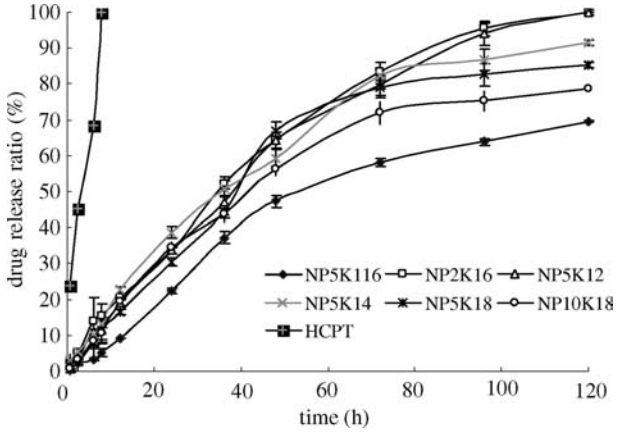

Fig. 4 In vitro release curve of HCPT–MePEG–PCL micelle and HCPT water solution

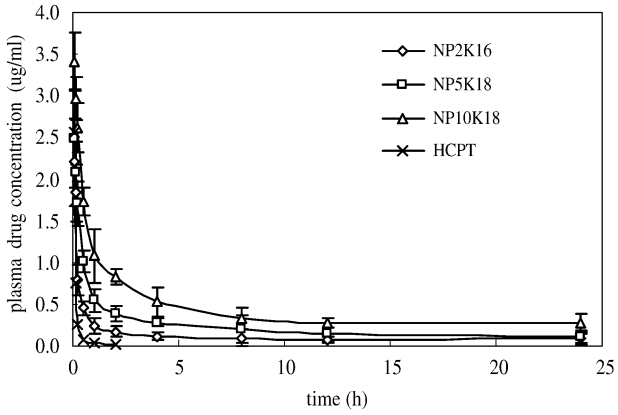

Fig. 5 Concentration–time curve of HCPT in rat plasma after i.v. administration of HCPT-MePEG-PCL-NP and HCPT (2.5 mg kg^{-1} body weight, $n = 6$)

($p < 0.05$). This may be due to the smaller particle size of the $MePEG_{10,000}$-PCL, which accelerated the drug release. On the other hand, the release rate of the drug was controlled by the PCL chain length. The release pattern showed that the longer the PCL chain length, the slower the drug release speed. In $MePEG_{5,000}$-PCL (1:2), the drug was totally released in 5 days while in $MePEG_{5,000}$-PCL (1:4), $MePEG_{5,000}$-PCL(1:8) and $MePEG_{5,000}$-PCL (1:16), the drug was released by 90, 85 and 70%, respectively ($p < 0.05$).

Compared to the HCPT-1 release from PCLLA–PEG–PCLLA micelles [32], the release of HCPT from MePCL-PEG micelle was quite slow. Torchilin reported that, with the increase of drug loading, some drugs might start to form crystals, which facilitate the micelles stability and reduce its drug release speed [1]. Our results of XRD showed that the micelles encapsulated lots of crystals of HCPT, which was consistent with that of Shenderova et al. [38] and Ertl et al. [40]. Furthermore, the hydrophobic core of MePEG-PCL has a higher *T*g, and the movement of small drug molecules in a relatively rigid glassy polymeric matrix is much harder than in a liquid core. What is more, the longer chain length of PCL could have bigger particle sizes, smaller particle surface area and thicker diffusion layer thickness, which also slowed down the drug release speed. At last, as fitted by Peppas equation shown in Table 3, Korsmeyer–Peppas exponent of all MePEG-PCL micelles were higher than 0.69, illustrating that the drug release was controlled by the diffusion and erosion mechanism.

Pharmacokinetics of micelles

The blood clearance curves for HCPT loaded in micelles after intravenous injection are shown in Fig. 5. The MePEG-PCL micelles showed initial higher blood circulating levels compared with free HCPT. In fact, the concentration of HCPT of $MePEG_{2,000}$-PCL, $MePEG_{5,000}$-PCL and $MePEG_{10,000}$-PCL in blood at 4 h after intravenous administration was about 5.01, 11.16, 23.92-fold than that observed for the free HCPT. And after 4 h, free HCPT was quickly removed from the circulating system and could not be detected. On the contrary, MePEG-PCL micelles exhibited a remarkable delayed blood clearance. It could be seen that the blood concentration of MePEG-PCL micelles remained higher after 24 h. The concentration–time curves for MePEG-PCL micelles and free HCPT in rats were fitted by the two-compartment model, and their pharmacokinetic parameters were shown in Table 4. The result showed that MePEG-PCL nanoparticles with PEG molecular weight of 2,000, 5,000, 10,000 could extend the half-life of HCPT to 4.54, 7.69, 16.54 h, respectively. Meanwhile, the AUC increased by 9.13, 13.82, 21.25-fold, compared to free HCPT solution.

Stolnik et al. [16] suggested that the effect of the surface modification on prolonged circulation would be limited to a relatively narrow size range of 70–200 nm. And Avgoustakis [36] confirmed that the poly(lactide-*co*-glycolide)-poly(ethylene glycol) (PLGA-PEG) micelles smaller than 70 nm could penetrate more efficiently through the fenestrae in the endothelial lining of the liver and associate with parenchymal cells. It was reported, however, that the pore size of tumor microvessels varies from 100 nm to 780 nm in diameter depending on the anatomic location of the tumor and the tumor growth [41]. Therefore, it was very ideal for the MePEG-PCL micelle size range from 70 nm to 100 nm (shown in Table 2) to maintain in the circulation and accumulate in body regions with leaky vasculature.

The in vivo characteristics of MePEG-PCL micelles were consistent with the micelles' in vitro physicochemical characteristics. As $MePEG_{10,000}$-PCL micelles had longer PCL chain length and possessed more

Table 4 Pharmacokinetics parameters of HCPT-MePEG-PCL-NP and HCPT solution in rats after i.v. administration

Parameters	NP2K16 Mean (SD)	NP5K18 Mean (SD)	NP10K18 Mean (SD)	HCPT Mean (SD)
$t_{1/2}\alpha$ (h)	0.0977 (0.0563)	0.1257 (0.0247)***	0.1738 (0.0560)***	0.0813 (0.0151)
$t_{1/2}\beta$ (h)	4.5441 (4.0505)*	7.6884 (3.2090)***	16.5360 (7.0385)***	0.7213 (0.2186)
AUC (h μg ml^{-1})	7.4953 (1.8110)***	11.3495 (3.2208)**	17.4490 (5.0221)***	0.821 (0.0946)
Cl (ml h^{-1})	0.2801 (0.0672)***	0.1486 (0.0963)***	0.1240 (0.0398)***	0.6160 (0.0729)
MRT (h)	3.3828 (1.2132)***	22.0909 (11.9530)***	33.1907 (10.5581)***	0.5883 (0.109)

*$p < 0.05$, **$p < 0.01$, ***$p < 0.005$ the data is compared between micelle group and HCPT

rigid structure, higher drug-loading coefficient, it was understandable that it would release drug more slowly and have a relatively longer half-life. Further, PEG density was crucial for the micelles' in vivo behavior. An optimal grafting surface density close to 0.67 and 0.5 PEG/nm^2 molecule for one PEG2000 was suggested for avoiding complement consumption by Bazile et al. [22]. In the proposed model, a grafting surface density of 0.18, 0.38 and 0.56 PEG/nm^2 was found for micelles of $MePEG_{10,000}$-PCL, $MePEG_{5,000}$-PCL and $MePEG_{2,000}$-PCL, respectively, corresponding to a distance between two PEG chains of 2.35, 1.34 and 1.62 nm. If we took the longer chain of PEG into consideration and the space it needed for its flexibility, it was quite reasonable that $MePEG_{10,000}$-PCL required less dense PEG surface density. And in terms of FALT, $MePEG_{10,000}$-PCL had the thickest FALT of 7.13 nm, nearly two times that of $MePEG_{2,000}$-PCL. These data confirmed that MePEG-

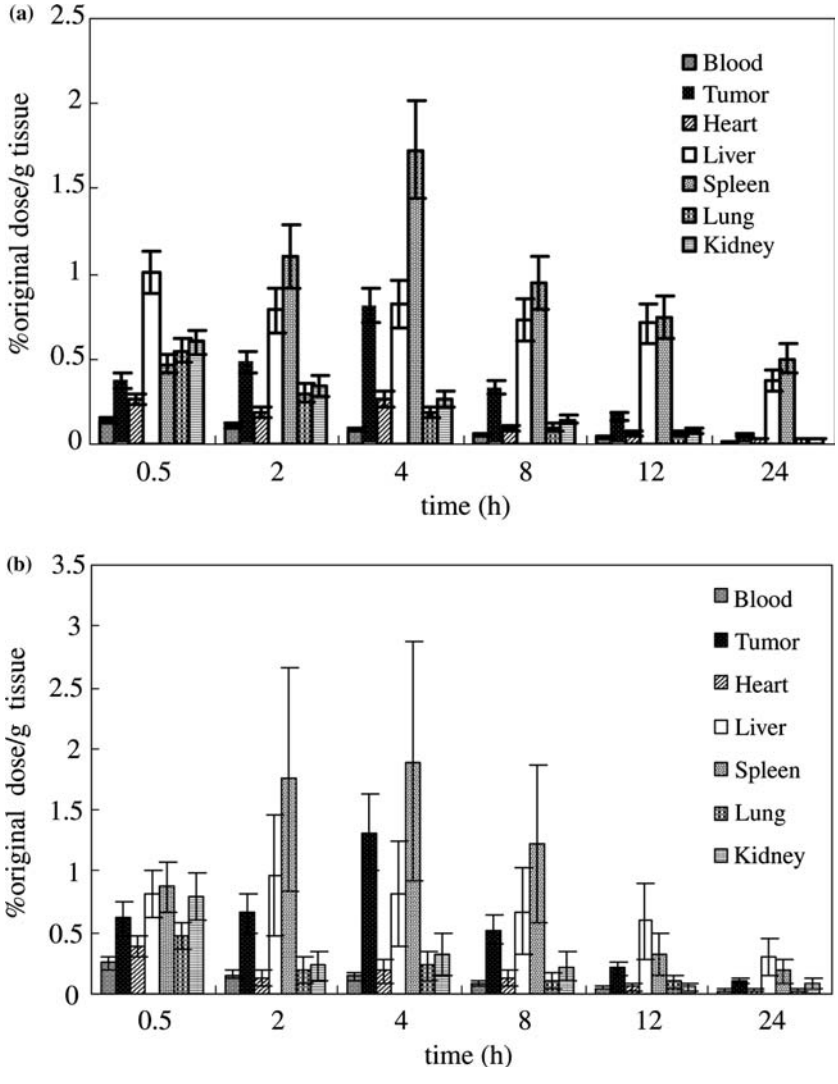

Fig. 6 Body distribution of ^{125}I-HCPT after i.v. administration of ^{125}I-HCPT-loaded micelles and ^{125}I-HCPT solution in mice: **a** $MePEG_{2,000}$-PCL, **b** $MePEG_{5,000}$-PCL, **c** $MePEG_{10,000}$-PCL, **d** free ^{125}I-HCPT solution

Fig. 6 (Contd.)

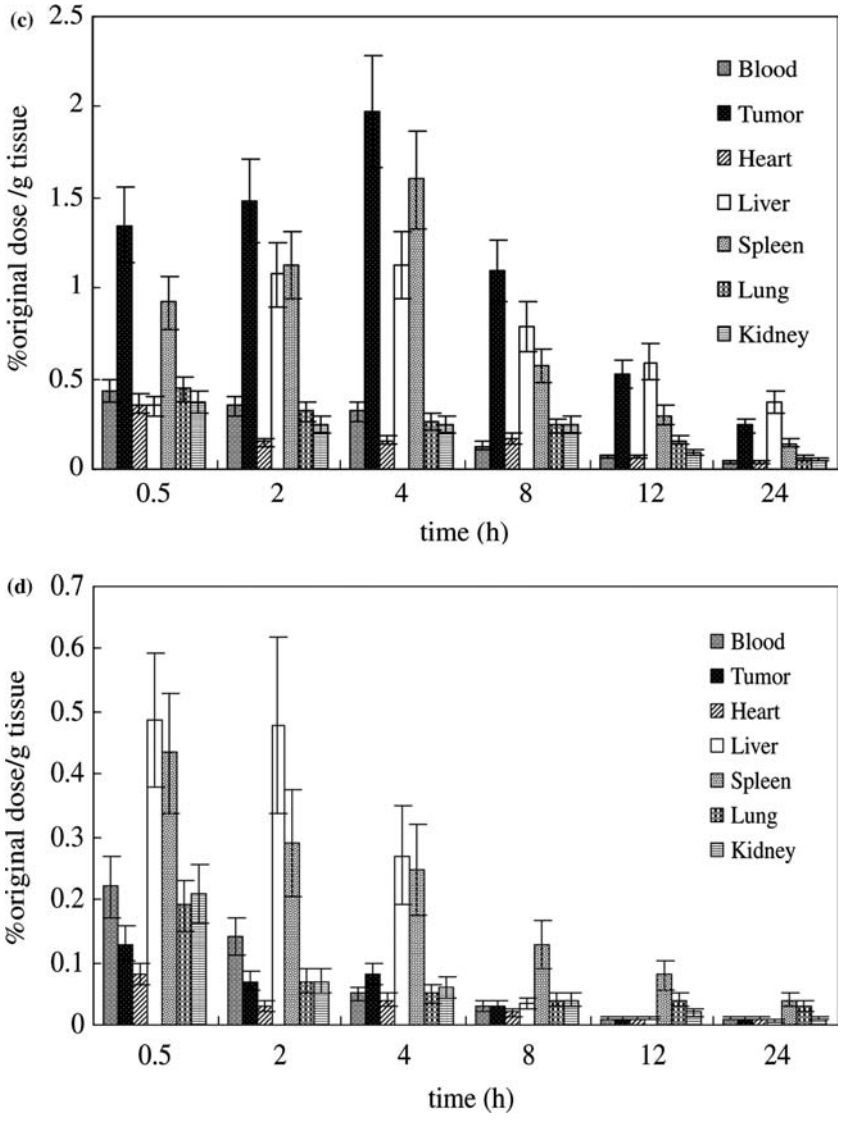

PCL micelle was enough to provide enhanced stability in the blood compartment to prevent the adsorption of various blood components onto their surface.

In conclusion, it was due to the longer PEG chain length, higher FALT and enough PEG surface density that led to best long-circulating properties of Me-PEG$_{10,000}$-PCL. This result was consistent with that of Gref's who supposed that a maximal increase in blood circulation half-time was found for a PEG molecular weight of 20,000 g/mol [42].

Table 5 Pharmacokinetics parameters of ^{125}I-HCPT-loaded micelles and ^{125}I-HCPT solution in tumor

Parameters	NP2K16[a] Mean (SD)	NP5K18[a] Mean (SD)	NP10K18[a] Mean (SD)	HCPT solution[b] Mean (SD)
$t_{1/2}k_e$ (h)	4.3920 (2.0629)***	3.6239 (1.6121)	5.5954 (0.6661)***	3.71 (0.67)
T_{max} (h)	2.8698 (0.1658)***	2.9244 (0.0825)***	2.5262 (0.0304)***	0.00
C_{max} (cpm/g)	134,266 (12,121)***	198,839 (17,948)***	380,945 (34,577)***	33,848 (4,397)
AUC (h cpm/g)	1,436,105 (126,769)***	2,047,848 (181,962)***	4,718,827 (425,083)***	180,940 (21,228)
CL (g/h)	0.1535 (0.0132)***	0.1076 (0.0093)***	0.0467 (0.0041)***	1.22 (0.15)
MRT[c] (h)	8.7424 (2.8987)***	9.5615 (2.1753)***	10.2677 (1.0529)***	5.69 (0.58)

$^{*}p<0.05$, $^{**}p<0.01$, $^{***}p<0.005$ the data is compared between micelle group and HCPT

[a]Pharmacokinetics parameters imitated by one compartment model: $X = k_a X_0/(k_a - k_e) \times \left(e^{-k_e t} - e^{-k_a t}\right)$

[b]Pharmacokinetics parameters imitated by one compartment model: $X = X_0 \times e^{-k_e t}$

[c]MRT got by statistical moments theory

Biodistribution of ^{125}I-HCPT in micelles and solution

The HCPT was successfully labeled by ^{125}I with a purity of 97% and it was quite stable when incubated with plasma for about 24 h (data not shown). Furthermore, the radioactivity measured in the thyroid tissue was very low, indicating that ^{125}I was not liberated from ^{125}I-HCPT. Therefore, it was quite reliable that the data got below could be attributed to the ^{125}I-HCPT.

Figure 6 shows the body biodistribution profiles of ^{125}I-HCPT in S_{180} tumor bearing mice that i.v. administered with ^{125}I-HCPT solution (Fig. 6d) and three samples of MePEG-PCL micelles, i.e. $MePEG_{2,000}$-PCL (Fig. 6a), $MePEG_{5,000}$-PCL (Fig. 6b) and $MePEG_{10,000}$-PCL (Fig. 6c). The relative radioactivity of ^{125}I-HCPT found in sampled tissues at each sampling point was expressed in percentage of the original dose per gram tissue. It was found that the blood concentration of free ^{125}I-HCPT was quite lower than that in micelles. We further compared that HCPT and ^{125}I-HCPT behavior in blood compartment and found ^{125}I-HCPT had a longer $t_{1/2}\beta$ of 1.5164 h while HCPT had a $t_{1/2}\beta$ of 0.7213 h. This illustrated that in vivo behavior of HCPT was different from that of ^{125}I-HCPT. Therefore, ^{125}I-HCPT was just used as a radioactivity probe to demonstrate the effects of MePEG-PCL on ^{125}I-HCPT. All data got below could not be attributed to HCPT.

Figure 6 shows that the tissue concentration of ^{125}I-HCPT in MePEG-PCL micelles remained relatively higher even at 24 h post injection, especially in tumor, spleen and liver. The free ^{125}I-HCPT was gradually eliminated from the tumor as shown by Fig. 6d. We imitated the tumor distribution behavior of free ^{125}I-HCPT applying the mathematic model of

$$X_t = X_0 \times e^{-k_e t} \tag{9}$$

suggesting that after time (t), the initial amount of ^{125}I-HCPT (X_0) was eliminated from the tumor at a speed coefficient of k_e, leading to the amount of ^{125}I-HCPT (X_t) at time (t). In this model, At the zero time of injection, its C_{max} in tumor was imitated at 33,848 cpm/g. However, in MePEG-PCL micelles, we could observed the rise of ^{125}I-HCPT in tumor during the first 4 h post injection. So we provided another mathematic model of

$$X_t = \frac{k_a X_0}{(k_a - k_e)} \times \left(e^{-k_e t} - e^{-k_a t}\right) \tag{10}$$

in which k_a was the speed coefficient of accumulation. In this model, we got that C_{max} of ^{125}I-HCPT in MePEG-PCL was about 3.97, 5.87 and 11.25 times that of free ^{125}I-HCPT, increasing with the increase of PEG chain length, while t_{max} was prolonged to about 2.5 h (shown in Table 5). This may be due to the long-circulating effects of the micelles and the filtration effect of the tumor capillary bed, namely the enhanced permeability and retention (EPR) effect. Unlike the normal and inflammatory tissues which proceeded rapidly and steadily via the lymphatic system, clearance of macromolecules and lipids from tumor was so impaired that they remained in the tumor interstitium for a longer time [41]. Therefore, it was possible for the MePEG-PCL micelles with sizes ranging from 80 nm to 200 nm to accumulate in tumor with leaky vasculature (shown in Table 5). With the higher concentration of ^{125}I-HCPT and longer time it remained in the blood compartment, it was understandable that AUC of ^{125}I-HCPT was in the order of $MePEG_{10,000}$-PCL > $MePEG_{5,000}$-PCL > $MePEG_{2,000}$-PCL (shown in Table 5).

Similarly, the relatively high ^{125}I-HCPT in spleen and liver could be explained by the filtration effect. The ^{125}I-HCPT in liver, a major RES organ, was even lower than spleen. According to Stolnik [16], when the size exceeded 200 nm, the accumulation of micelles in liver was overwhelming and when the size was below 200 nm, the spleen was more powerful to catch the micelles because of its tighter structure. This could explain the higher filtration effect of spleen towards MePEG-PCL micelles smaller than 100 nm and represented an interesting possibility for spleen targeting of active molecules.

^{125}I-HCPT in kidney, one of the major elimination pathways of the original HCPT, was low. Furthermore, ^{125}I-HCPT in lung was low indicating that no obvious aggregates of MePEG-PCL could be observed, for particles size bigger than 5 μm could be readily filtrated by lung capillary bed. ^{125}I-HCPT in heart was lowest in all organs no matter in its free solution or in MePEG-PCL micelles, which would be responsible for the drug's lower heart toxicity.

A number of authors had reported that PEG-grafted micelles had long-circulating effects in vivo. Mosqueira confirmed that reduced uptake of liver and spleen could be responsible for the [^{3}H]-PLA-PEG nanocapsules' long circulating effects in the blood compartment [33]. Avgoustakis further probed into the copolymer composition on the biodistribution of ^{125}I-PLGA-PEG and found that the surface property and size of the micelle was associated with its biodistribution [36]. However, these experiments were carried out with no drug loaded and could not demonstrate the drug's interaction with the copolymer and the drug's behavior in vivo. In this article, we used ^{125}I-HCPT as a probe and compared the biodistribution behavior of ^{125}I-HCPT in MePEG-PCL micelles and in its free form.

In conclusion, by using the compartment model, we evaluated the tumor targeting effect of the MePEG-PCL micelles. It was due to the steric stabilization of PEG shell and small particle size that MePEG-PCL micelles could maintain in the blood long enough and accumulate in the tumor. More detailed in vivo study on this

drug delivery including its pharmacological effects is currently under further investigation.

Conclusion

It was illustrated in this work that the longer PCL chain length would lead to the reduction of CAC value, the increase of drug-loading coefficient, stabilized HCPT, sparser PEG surface density, and slower drug release patterns. On the other hand, the longer PEG chain length would lead to less negative zeta potential and larger fixed aqueous layer thickness, as well as the stabilized HCPT and sparser PEG surface density. These physicochemical parameters contributed together to the in vivo pharmacokinetic characteristics of MePEG-PCL micelles. We supposed that $MePEG_{10,000}$-PCL should be the best material for the purpose of prolonging the drug's circulation time. In this test, it could extend the half-life of HCPT to 16.54 h, almost 23 times that of free HCPT. At last, the accumulation of the ^{125}I-HCPT in tumor was significant due to EPR effect. It is promising that the change of pharmacokinetic characteristics of HCPT would lead to more powerful antitumor activity and less toxicity of the drug [43, 44]. This work established the foundation for further studies on the in vivo experiment of the MePEG-PCL micelles.

Acknowledgements This work was supported by the Shanghai Science and Technology Development foundation of Shanghai, PR China, No.0243nm067. We thank professor Huang Junlian for donation of $MePEG_{10000}$ and the assistance and instruction of professor Lu Jianzhong for characterization of the micelle. Finally, the HCPT was labeled as a probe by professor Zhu JiangHua.

References

1. Torchilin VP (2001) J Control Release 73:137
2. Brigger I, Dubernet C, Couvreur P (2002) Adv Drug Deliv Rev 54:631
3. Otsuka H, Nagasaki Y, Kataoka K (2003) Adv Drug Deliv Rev 55:403
4. Gabizon AA (1995) Adv Drug Deliv Rev 16:285
5. Storm G, Belliot SO, Daemen T, Lasic DD (1995) Adv Drug Deliv Rev 17:31
6. Maeda H, Wu J, Sawa T, Matsumura Y, Hori K (2000) J Control Release 65:271
7. Stella B, Arpicco S, Peracchia MT (2000) J Pharm Sci 89:1452
8. Li YP, Pei YY, Zhou ZH, Zhang XY, Gu ZH, Ding J, Zhou JJ, Gao XJ (2001) J Control Release 71:287
9. Li YP, Pei YY, Zhou ZH, Zhang XY, Gu ZH, Ding J, Zhou JJ, Gao XJ, Zhu JH (2001) Biol Pharm Bull 24:662
10. Cammas S, Suzuki K, Sone C, Sakurai Y, Kataoka K, Okano T (1997) J Control Release 48:154
11. Yokoyama M, Miyauchi M, Yamada N, Okano T, Kataoka K, Inoue S (1990) Cancer Res 50:1693
12. Ramaswamy M, Zhang X, Burt HM, Wasan KM (1997) J Pharm Sci 86:460
13. Jeong YJ, Cheon JB, Kim SH, Nah JW, Lee YM, Sung YK, Akaike T,Cho CS (1998) J Control Release 51:169
14. Zhou SB, Deng XM, Yang H (2003) Biomaterials 24:3563
15. Kim SY, Lee YM, Shin HJ, Kang JS (2001) Biomaterials 22:2049
16. Stolnik S, Illum L, Davis SS (1995) Adv Drug Deliv Rev 16:195
17. Gref R, Domb A, Quellec P, Blunk T, Muller RH, Verbavatz JM, Langer R (1995) Adv Drug Deliv Rev 16:215
18. Allen C, Maysinger D, Eisenberg A (1999) Coll Surf B Biointerf 16:1
19. Gref R, Luck M, Quellec P, Marchand M, Dellacherie E, Harnisch S, Blunk T, Muller RH (2000)Coll Surf B Biointerf 18:301
20. Mosqueira VCF, Legrand P, Morgat JL, Vert M, Mysiakine E, Gref R, Devissaguet JP, Barratt G (2001) Pharm Res 18:1411
21. Sadzuka Y, Nakade A, Hirama R, Miyagishima A, Nozawa Y, Hirota S, Sonob T (2002) Int J Pharm 238:171
22. Bazile D, Prud'Homme C, Bassoulet MT, Marlard M, Spenlehauer G, Veillard M (1995) J Pharm Sci 84:493
23. Vittaz M, Bazile D, Spenlehauer G, Verrecchia T, Veillard M, Puisieux F, Labarre D (1996) Biomaterials 17:1575
24. Li YF, Zhang RW (1996) J Chromatogr B 686:257
25. Rowinsky E, Grochow L, Hendricks CB, Ettinger D, Forastier AA, Horowitz LA, Donehower DC (1992) J Clin Oncol 10:647
26. Kwon G, Yokoyama M, Okano T, Sakurai Y, Kataoka K (1993) Pharm Res 10:970
27. Cortesi R, Esposito E, Maietti A, Menegatti E, Nastruzzi C (1997) Int J Pharm 159:95
28. Yang SC, Lu LF (1999) J Control Release 59:299
29. Ryu JG, Jeong YJ, Kim IS, Lee JH, Nah JW, Kim SH (2000) Int J Pharm 200:231
30. Marctic PA, Nair M (1994) J Coll Interf Sci 163:517
31. Peracchia MT, Vauthier C, Passirani C, Couvreur P, Labarre D (1997) Life Sci 61:749
32. Zhang LY, Hu Y, Jiang X, Yang CZ, Lu W, Yang YH (2004) J Control Release 96:135
33. Manosroi A, Wongtrakul P, Manosroi J, Sakai H, Sugawara F, Yuasa M, Abe M (2003) Coll Surf B Biointerf 30:129
34. Riley T, GovenderT, StolnikS, Xiong CD, Garnett MC, Illum L, Davis SS (1999) Coll Surf B Biointerf 16:147
35. Yamamoto Y, Nagasaki Y, Kato Y, Sugiyama Y, Kataoka K (2001) J Control Release 77:27
36. Avgoustakis K, Belestsi A, Panagi Z, Klepetsanis P, Livaniou E, Evangelatos G, Ithakissios DS (2003) Int J Pharm 259:115
37. Needham D, Stoicheva N, Zhelev DV (1997) Biophys J 73:2615
38. Shenderova A, Burke TG, Schwendeman SP (1997) Pharm Res 14:1406
39. Burke TG, Mi Z (1993) J Med Chem 36:2580
40. Ertl B, Platzer P, Wirth M, Gabor F (1999) J Control Release 61:305
41. Jang SH, Wienties MG, Lu D, Au L (2003) 20:1337
42. Gref R, Minamitake Y, Peracchia MT, Trubetskoy V, Torchilin V, Langer R (1994) Science 263:1600
43. Hatefi A, Amsden B (2002) Pharm Res 19:1389
44. O'Leary J, Muggia FM (1998) Eur J Cancer 34:1500